

Науки о Земле Earth sciences

УДК 550.8+550.34+ 553.98

<https://doi.org/10.21440/2307-2091-2019-3-7-19>

Three-dimensional depth-based structural modelling of the central eastern part of the Gulf of Suez, Egypt

Ahmed TARSHAN^{1, 2*}

Sergey Vladimirovich SHIMANSKIY^{1**}

Mamdouh M. ABDEEN^{3***}

¹Saint Petersburg State University, Saint Petersburg, Russia

²Nuclear Materials Authority, Cairo, Egypt

³National Authority for Remote Sensing and Space Sciences, Cairo, Egypt

Building a three dimensional (3D) geological model of field and subsurface data is an important task in geological and geophysical studies.

The goal of this research is to build 3D structural model of the central eastern part of the Gulf of Suez, Egypt. Available seismic sections and well data were collected for use in building the model. Each horizon, on each seismic section, was digitised accurately using Petrel software for generating a depth-structure map for each horizon. The basement layer was constructed using airborne magnetic data of the area under study. The GM-SYS-3D inversion code was used to presume the sedimentary section-basement complex magnetic susceptibility. Estimates of the depth to the basement varied reliably between 500 and 4700 m. Data from 24 drilled wells within the area was used to define the thickness and orientation of the layers between the horizons of the 3D grid model. A model consisting of 29 layers, including the topography and basement layers, was created using Petrel software.

Results of the 3D model show that the study area has a multi-reservoir character, with several productive pre-rift and synrift reservoirs. It contains seven reservoirs overlain by sealing rocks and underlain by source rocks. The presence of hydrocarbons in these reservoirs has been demonstrated in some fields in the area. Five new locations are also recommended for detailed 2D and 3D seismic survey, as hydrocarbon may be present in these locations.

Keywords: 3D modelling, depth-structure maps, horizons and layering, Gulf of Suez, Egypt.

Introduction

The Gulf of Suez (GOS) is the northwestern arm of the Red Sea rift system and partly separates the Sinai Peninsula from the remainder of Egypt (Fig. 1). It is a Cenozoic rift about 300 km long and up to 80 km wide. Uplift of both flanks of the rift exposed a relatively complete stratigraphic section ranging in age from the Precambrian to the Quaternary (Fig. 2). Exposures are excellent, with arid climate and active erosion allowing a detailed and clear examination of the sedimentological, stratigraphical and structural relationships [1–3].

The pre-rift sedimentary sequence is composed of strata ranging in age from Cambrian to Late Eocene and contains sand, shale, and carbonate facies that were laid down over the Precambrian granitic basement under terrestrial and marine platform environments. This period of sedimentation was affected by major unconformities representing non deposition or erosion at different geologic times [5]. The Phanerozoic stratigraphic sequence is composed of the Nubia Group (Nubia D, Nubia C, Nubia B, and Nubia A formations), Raha, Abu Qada, Wata, Matulla, Dawi (Brown limestone), Sudr, Esna, and Thebes formations (Fig. 3).


The syn-rift stratigraphic sequence in the GOS is composed of Miocene strata ranging in age from (29.3–13 Ma). It is represented by Nukhul, Rudeis and Kareem formations (Fig. 3).

The post-rift stratigraphic sequence in the GOS is represented by strata ranging in age from (14.2–0 Ma) [6]. This sequence is represented by Belayim, South Gharib, and Zeit formations (Fig. 3).

The GOS is the most prolific and prospective oil province in Egypt, and any open acreage, or relinquished areas, will be of great interest to the oil industry. The majority of oil fields in the GOS incorporate multiple productive reservoirs. These reservoirs can be classified as (1) pre-rift reservoirs, such as the Precambrian fractured granitic rocks, Palaeozoic–Lower Cretaceous Nubian sandstones, Upper Cretaceous Nezzazat sandstones and the Eocene fractured Thebes limestone; (2) synrift reservoirs, such as the Miocene sandstones and carbonates of the Nukhul, Rudeis, Kareem, and Belayim formations and the sandstones of South Gharib, Zeit, and post-Zeit formations. Miocene evaporites are the ultimate hydrocarbon seals, and the shale and dense limestones of the pre-rift and the synrift stratigraphic units are the primary seals [5]. Structural, stratigraphical, and combination traps are encountered in the study area.

A large number of reservoir models can be created relatively quickly with geostatistical tools, such as Petrel modelling software; one of the most popular modelling software in oil industry, but often a limited number of inputs must be selected to the flow simulation due to computational time requirements [7]. 3D modelling is the process of developing a mathematical representation of any 3D surface of object (either inanimate or living) via specialised software. The product is called a 3D model [8, 9]. In general, the model is a representation of something, or an event in the real world. The model is good if it adequately describes a property or some real world properties relevant to the study. For example, a 3D geological model of an area is good if it returns the values of the real world in reservoir simulations and reservoir modelling.

* ahmed_ramadan_geo@hotmail.com

 <https://orcid.org/0000-0001-9710-9392>

** s.shimanskii@spbu.ru

 <https://orcid.org/0000-0002-5403-5220>

*** mamdouh.abdeen@narss.sci.eg

 <https://orcid.org/0000-0001-8863-1322>

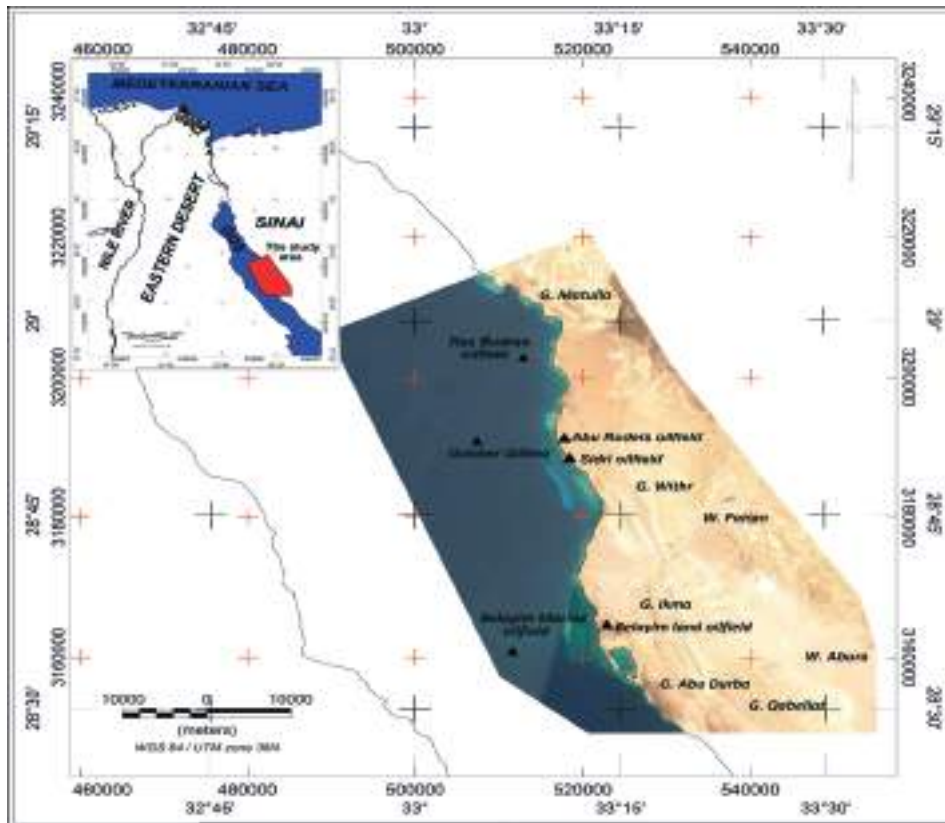


Figure 1. Location map and satellite image of the study area, with the location of main features and oil fields.
 Рисунок 1. Карта расположения и спутниковое изображение области исследования, с расположением основных особенностей и нефтяных месторождений.

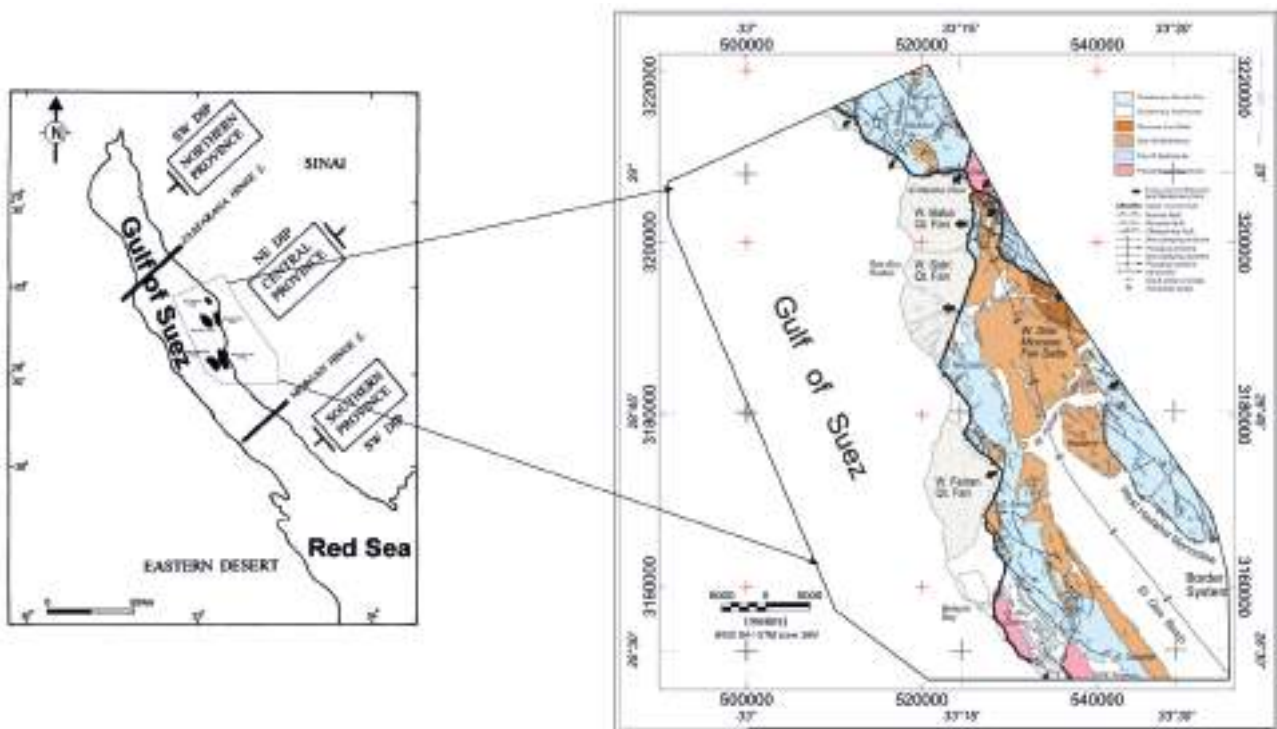


Figure 2. Geological map of the central eastern part of the Gulf of Suez, Egypt [4]. The onset map shows the Gulf of Suez, the three dip provinces and the hinge (accommodation) zones between them and the location of main oil fields.
 Рисунок 2. Геологическая карта центрально-восточной части Суэцкого залива, Египет [4]. На карте изображен Суэцкий залив, три провинции с наклоном и зоны пластичности между ними, а также показано расположение основных нефтяных месторождений.

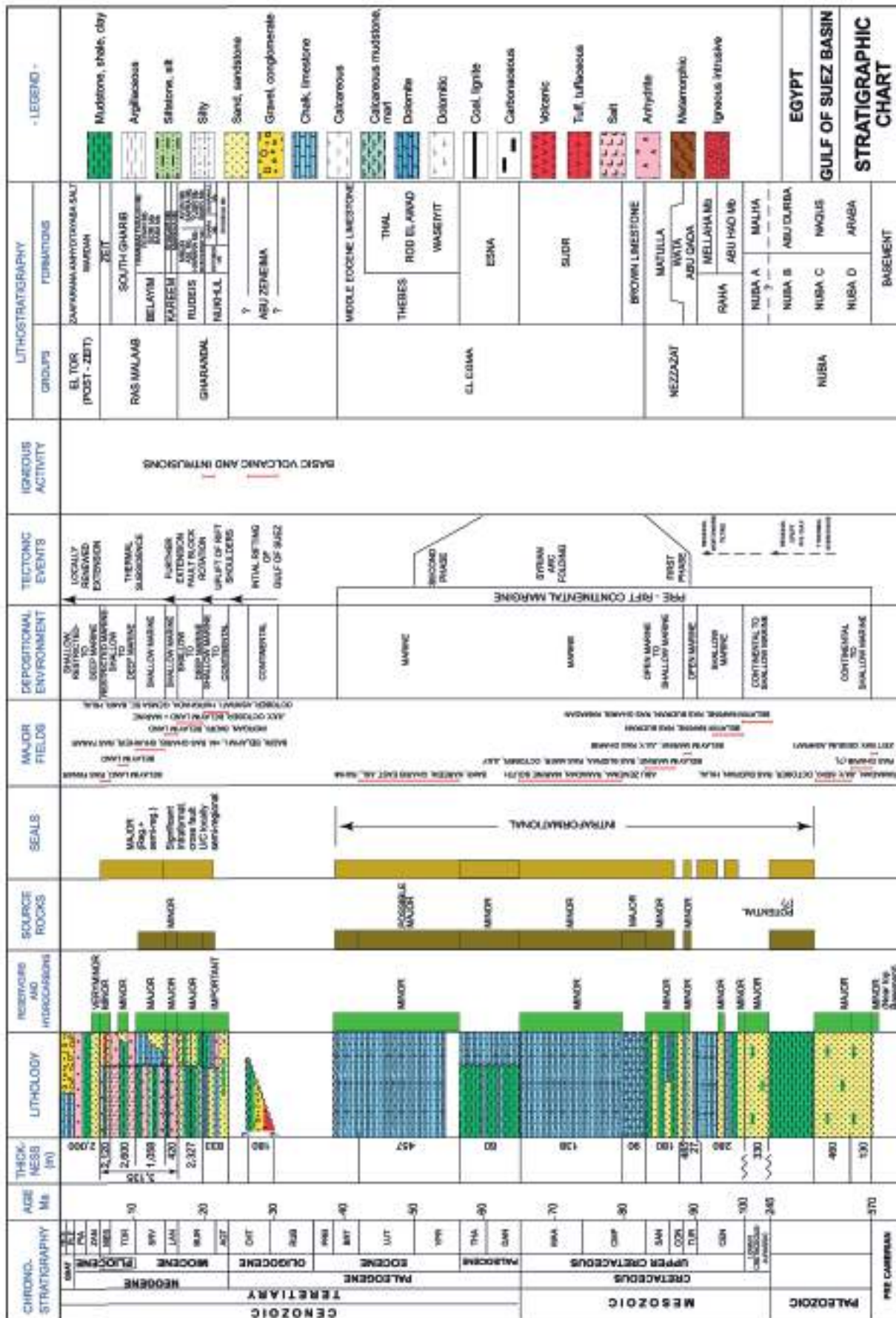


Figure 3. Litho-stratigraphic column of Gulf of Suez [6].
Рисунок 3. Литостратиграфический разрез Суэцкого залива [6].

In this research, a 3D model of the central eastern part of the GOS rift (Fig. 1) was built using seismic and well data as well as airborne magnetic data and surface digital elevation model (DEM).

The study area covers 2745 km² and lies between latitudes 28°28'07.22" and 29°06'46.05" North and longitudes 32°54'27.39" and 33°33'44.13" East. Data was collected and digitised using Petrel software to be used in building the model. 3D modelling of the airborne magnetic data was performed to delineate the basement relief. Structure depths maps were created using seismic and well data. The study area includes five well known oil fields (Fig. 1); from north to south, are Ras Budran, Abu Rudeis, October, Feiran and Belayim.

1. 3D magnetic modelling

In March 1998, the Airborne Geophysics Department of the Nuclear Materials Authority (NMA) of Egypt led a high-resolution aeromagnetic survey covering 2745 km² over the central eastern part of the GOS. Data was gained along primary (essential) lines spaced at 1000 m, and along control lines spaced at 10000 m, (normal to the primary lines). The nominal flying elevation was about 100 m (330 ft) above the ground surface (terrain clearance). The direction of the survey was 125°–305° azimuth degrees for the primary lines and 35°–215° azimuth degrees for the control lines.

Using the GM-SYS-3D inversion code, the presumed sedimentary section-basement complex magnetic susceptibility contrast Δk for several inversion trials was gradually set between 0.035 and 0.08 SI during the inversion run. The inverted basement relief images, corresponding to the used susceptibility contrasts, were consistently inspected. The effective susceptibility contrast was found to be close to the susceptibility contrast of 0.0628 SI (5000 micro cgs unit), and accordingly, its calculated basement relief image was established (Fig. 4). The overall calculated 3D response fits the observed geomagnetic data (better than ± 50.0 nT). Other model parameters are set to be constant for all trails (convergence limit: 10 nT, Z0: 0m and regional offset: 0.0), where Z0 is the nominal top of the basement surface. Estimates of the depth to the basement varied between 500 and 4700 m. The basement relief encountered at the study area has shown three major basinal structures (Fig. 4). These basins are located at the northwestern, west central and southeastern parts of the study area [10].

2. Creating depth-based structural model

The available interpreted seismic sections and well data in the area under study were collected from different published sources [11–13]. Sixteen seismic sections were obtained covering the northern, central and southern parts of the study area in addition to a single geologic cross section for the southeastern part of the area (Fig. 5). Seismic lines GS-370, in-line 195, in-line 215, in-line 215, cross-line 360, cross-line 280 and cross-line 330 are published by [12]. Seismic lines RG-12-82, RG-14-82, RS-27-83, R6-05-82, and R6-07-83 are published by [13]. Seismic lines 1330, 1150, 1570 and ARB are published by [11]. The geologic cross section for the southeastern part of the study area is obtained from [14]. These data were gathered and used in producing a depth-structure map for each formation in the area under study using Petrel software. The locations of these lines were traced accurately from the location map of the area (Fig. 5); the longitude and latitude were defined for each line and were used in locating the seismic lines in their exact locations in the 3D view (Fig. 6) [15].

2.1. Data digitising

Each horizon on each seismic section was digitised accurately using Petrel software to be used in creating a depth-structure map for the top of each horizon, as shown in Fig. 7, a–f. These figures show the intersection between the depth-structure maps

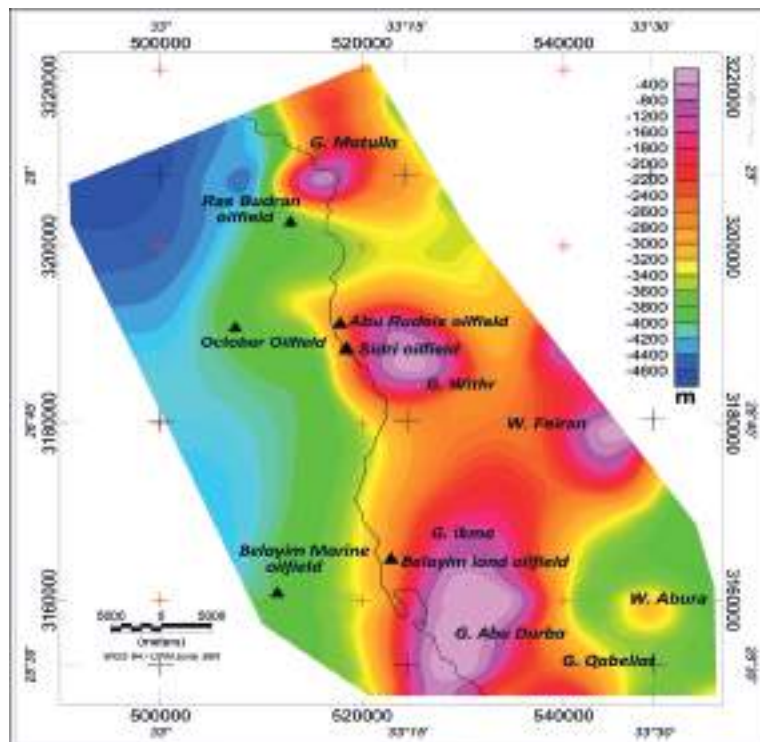


Figure 4. Basement relief contour map of the study area using aero-magnetic data after performing the 3D layered-earth inversion of the subsurface magnetic susceptibility distributions [10].

Рисунок 4. Контурная карта рельефа фундамента исследуемой территории с использованием аэромагнитных данных после проведения трехмерной инверсии слоистой среды приповерхностных распределениях магнитной восприимчивости [10].

of the top of each formation and the seismic sections. For example, Fig. 7, a illustrates the intersection between the produced depth-structure map of the top South Gharib Formation with seismic line RG-12-82. These figures indicate that there is an adequate matching between the digitised seismic sections and the depth-structure maps.

2.2. Well data

Depth to each formation was gathered from different wells in the area under study from different published sources [15–24] as shown in Table. The locations of the all wells are illustrated in Fig. 5. These data were plotted on the 3D view using Petrel software (Fig. 6).

2.3. Depth-structure maps

One of the most important tools for 3D structural interpretation is the structure contour map. This is because it is seen as a fully 3D form of the map horizon. The well data and the digitised horizons were used together to create depth-structure maps for the main horizons using Petrel software. Nine depth-structure maps were generated for Zeit, South Gharib, Belayim, Kareem, Rudeis, Nukhul, Thebes, Matulla and Nubia formations (Fig. 8, 9, 10, a). The topographic map (Fig. 10, b) of the study area was produced using Shuttle Radar Topography Mission (SRTM) data and Geosoft Oasis Montaj. The data is uploaded in the three dimensional view using Petrel software (Fig. 12).

2.4. Pillar Gridding

It is the process of creating the grid that is the basis of all 3D modelling. The skeleton of the model consists of upper, middle and base skeleton grids. The produced pillar gridding using Petrel software is shown in Fig. 11.

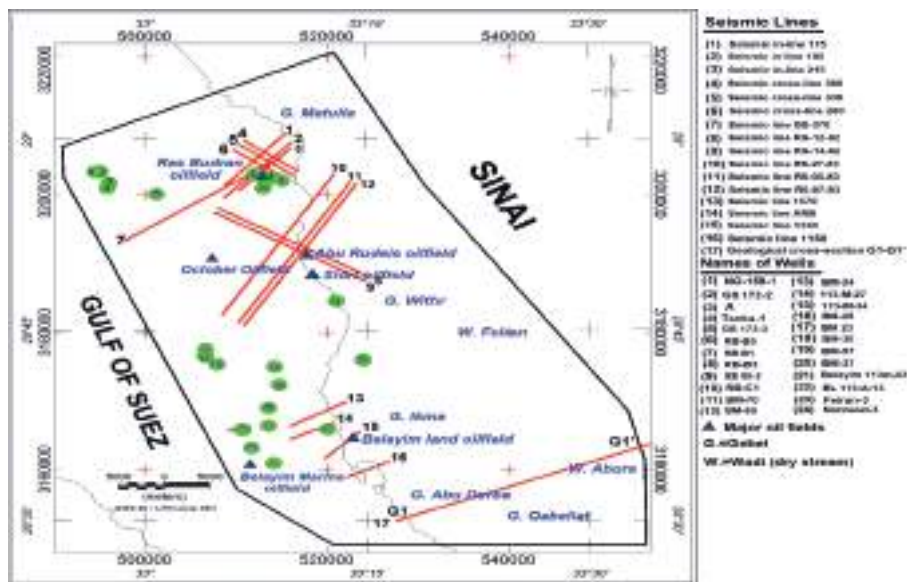


Figure 5. Location map of wells and seismic sections used in the model building, eastern part of Gulf of Suez [15].
 Рисунок 5. Карта расположения скважин и сейсмических разрезов, использованных в модельном построении восточной части Суэцкого залива [15].

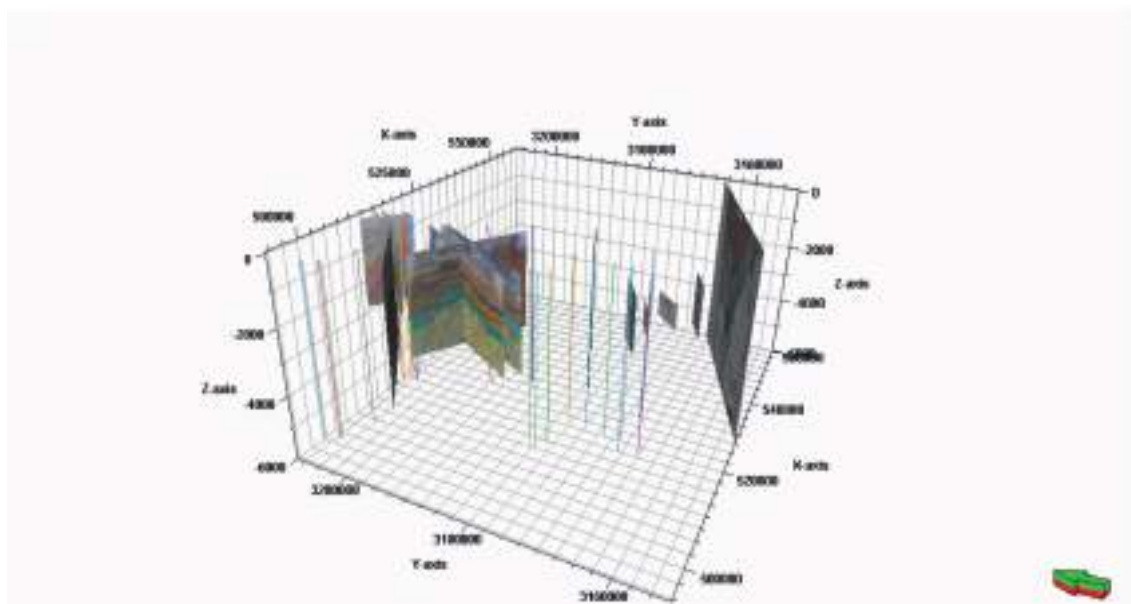


Figure 6. Three dimensional view using Petrel software illustrating the location of the wells and the seismic lines used in the model construction.
 Рисунок 6. Трехмерное изображение с использованием программного обеспечения Petrel, иллюстрирующее местоположение скважин и сейсмических линий, используемых при построении модели.

Table 1. Depth in meters to top of each layer in wells (A, NO-159-1, GS 172-2, GS 173-3, RB-B5, RB-B1, RB-B3, EE 85-2, RB-C1, Tanka-1, BM-30, BM-37, Belayim 113m-63, Feiran-3, Nazzat-3, BM-70, BM-65, BM-24, 113-M-27, 113-M-34, BM-29, BM 23, BM-57, BL 113-A-15) in the central eastern part of the Gulf of Suez, Egypt.
Таблица 1. Глубина в метрах до кровли каждого пласта в скважинах (А, NO-159-1, GS 172-2, GS 173-3, RB-B5, RB-B1, RB-B3, EE 85-2, RB-C1, Tanka-1, BM-30, BM-37, Belayim 113m-63, Feiran-3, Nazzat-3, BM-70, BM-65, BM-24, 113-M-27, 113-M-34, BM-29, BM 23, BM-57, BL 113-A-15) в центральной восточной части Суэцкого залива, Египет.

Layer Name	A	NO-159-1	GS 172-2	GS 173-3	RB-B5	RB-B1	RB-B3	EE 85-2	RB-C1	Tanka-1	BM-30	BM-37	Belayim 113m-63	Feiran-3	Nazzat-3	BM-65	BM-24	113-M-27	113-M-34	BM 23	BM-57	BL 113-A-15	BM-29	BM-70
Zeit FM.	-	975.3	853.44	-	949.14	938.78	935.12	847.34	900.98	-	-	-	-	-	489.2	840	809	1146	1104	1033	835	-	-	1067
South Garhib FM.	-	1950.7	1981.2	-	1359.7	1333.2	1327.7	1362.15	1269.5	-	-	-	-	1148.79	-	1626	1446	1896	1844	1711	1500	-	-	1899
Hammam Faroun Mbr. (including three beds forming trap)	-	2179.3	2255.52	1645.92	1623.4	1563.7	1570.3	1605.07	1551.1	-	-	-	-	-	-	2164	1978	2410	2404	2197	2002	-	-	2362
Feiran Mbr.	-	-	-	-	1663	1613.6	1606.9	1639.51	1565.1	-	-	-	-	-	-	-	2011	2469	2466	-	-	-	-	-
Sidi Mbr.	-	-	-	-	1805.9	1738	1733.4	1766.01	1741.6	-	-	-	-	-	-	-	2078	2576	2567	-	-	-	-	-
Baba Mbr.	-	-	-	-	1838.9	1769.7	1764.5	1791.61	1775.5	-	-	-	-	-	-	-	2097	2603	2592	-	-	-	-	-
Kareem-Shale Mbr.	2650	2438.4	2560.3	2133.6	1885.8	1820.3	1814.8	1842.51	1830	-	-	-	-	-	-	2667	2183	2710	2698	2503	2247	-	-	2592
Kareem-Mia Mbr.	-	-	-	-	2014.1	1912.9	1910.2	1952.49	1953.5	-	-	-	-	-	-	-	2373	2929	2919	-	-	-	-	-
Upper Rudais Mbr.	-	2621.2	2834.6	2712.7	2108.6	1998.6	1987.9	2058.61	2032.7	-	2865	2800	-	-	-	2811	2410	2919	2919	2686	2424	-	-	2792
Lower Rudais Mbr.	-	-	-	-	2605.4	2517	2377.7	2747.46	2606.3	-	-	-	-	-	-	-	2590	3331	3175	-	-	-	-	-
Nukhul FM.	-	3505.2	-	3322.2	3091.9	2517	2457.9	2747.46	3014.2	3728.61	-	-	-	-	-	3030	2590	3331	3175	2859	2565	-	-	3263
Thebes FM.	-	-	-	2922	3091.9	2517	2468.6	2777.33	3179.7	-	3000	-	2760	-	-	3030	2590	3331	3175	2922	2590	3051	-	3263
Ezna FM.	-	-	-	-	3091.9	2850.2	2872.1	3140.04	3298.2	-	-	-	-	-	-	-	2590	3568	3219	-	-	-	-	-
Sudr FM.	-	-	-	-	3091.9	2894.1	2909.3	3183.33	3311	-	-	-	-	-	-	-	2590	3572	3244	-	-	-	-	-
Dawi FM.	-	-	-	-	3091.9	2993.1	2950.5	3250.38	3311	-	-	-	-	-	-	-	2590	3572	3307	-	-	-	-	-
Matulla FM.	-	-	-	-	3091.9	3019	2988.3	3317.44	3311	-	-	-	3000	-	-	3124	2590	3587	3353	3085	2772	3397	-	3387
Wata-Qada FMs.	-	-	-	-	3196.7	3052.3	3105	3401.56	3311	-	-	-	-	-	-	-	2682	3715	3472	-	-	-	-	-
Raha FM.	-	-	-	-	3292.8	3191.3	3264.7	3446.98	3349.8	-	-	-	-	-	-	-	2775	3803	3559	-	-	-	-	-
Nubia A-P1 Mbr.	-	-	-	3808.78	3417.4	3337	3272	3560.36	3517.7	-	-	-	3140	-	-	3124	2834	3907	3657	-	2933	-	-	3615
Nubia A-S1 Mbr.	-	-	-	-	3426.3	3407.4	3393.3	3626.2	3543.3	-	-	-	-	-	-	-	2875	3933	3701	-	-	-	-	-
Nubia A-P2 Mbr.	-	-	-	-	3442.4	3428.7	3528.1	3639.92	3566.8	-	-	-	-	-	-	-	2916	3978	3820	-	-	-	-	-
Nubia A-S2 Mbr.	-	-	-	-	3514.95	3497.9	3565.6	3656.99	3603	-	-	-	-	-	-	-	2923	4002	3842	-	-	-	-	-
Nubia A-P3 Mbr.	-	-	-	-	3604.6	3552.4	3695.4	3759.7	3615.5	-	-	-	-	-	-	-	3005	4002	3842	-	-	-	-	-
Nubia A-S3 Mbr.	-	-	-	-	3604.6	3552.4	3695.4	3822.8	3615.5	-	-	-	-	-	-	-	3005	4002	3842	-	-	-	-	-
Nubia B FM.	-	-	-	-	3604.6	3552.4	3695.4	3822.8	3615.5	-	-	-	-	-	-	-	3005	4002	3842	-	-	-	-	-
Nubia C-D FM.	-	-	-	-	3604.6	3685.9	3695.4	3822.8	3750	-	-	-	-	-	-	-	3094	4121	4007	-	-	-	-	-
Basement	-	-	-	-	3746.6	3668.8	3785	4126.68	3652.7	-	-	-	-	-	-	-	3177	4181	4160	-	-	-	-	-
Reference	[16]	[17]	[18]	[19]	[20]	[21]	[22]	[23]	[24]															

2.5. Defining Horizons and Layering

The most important step in structural modelling is inserting the horizons into the pillar grid. The horizon process step was used to define the vertical layering in the 3D grid in Petrel software. The final step in building the structural framework is defining the thickness and orientation of the layers between the horizons of the 3D grid. Data was collected for 24 wells within the study area. The stratigraphic succession was defined from this data. This data shows that the study area consists of more than eleven layers as interpreted in the seismic sections. The seismic sections and the wells data were used to define the thickness and orientation of layers between horizons of the 3D grid.

Some formations are divided into members, for example, the Belayim Formation is divided into four members: Hammam Faroun, Feiran, Sidri and Baba. The Hammam Faroun Member includes three types of lithology: shale in the upper part of the member, sandstone in the middle and shale in the lower part, these lithologies form the trap in Belayim Formation. The Kareem Formation is divided into two members, Shale member that is composed of shale in the upper part of the formation and Ma member that is composed of anhydrites in the lower part of the formation. The Rudeis Formation is divided into Upper Rudeis and Lower Rudeis members. Four layers were generated between the horizons of the Thebes and Matulla, as follows: the Thebes, Esna, Sudr, and Dawi formations. Three layers were generated between the horizons of the Matulla Formation (Lower Senonian) and Nubia Formation. These layers are, the Matulla, Wata-Qada and Raha formations. Finally, the Nubia Formation is divided into seven layers, the Nubia A-P1, Nubia A-S1, Nubia A-P2, Nubia A-S2, Nubia A-P3, Nubia A-S3, and Nubia C-D.

The depth to the top of each formation is illustrated for all wells (Table), these depths data were used to manage the process of the layering, and the locations of these wells are illustrated in Fig. 5. Finally, a 3D depth model was created (Fig. 12).

Results and Discussion

The 3D model (Fig. 12) illustrates that the study area contains promising locations for hydrocarbon exploration; these locations are characterised by a good succession of sedimentary rocks overlying the basement layer. These rocks include the three types of rocks, source, reservoir and sealing rocks, to form traps. The petroleum system event chart (Fig. 13) of the area illustrates the source, reservoir and seal rocks with geological time, which indicate a possibility of traps forming in the area under study. However, the area includes five oil fields: Ras Budran field in the north central part, Abu Rudeis field to the south of Ras Budran field, Feiran field in the central part and the Belayim field in the southwestern part of the area. The probability of hydrocarbon po-

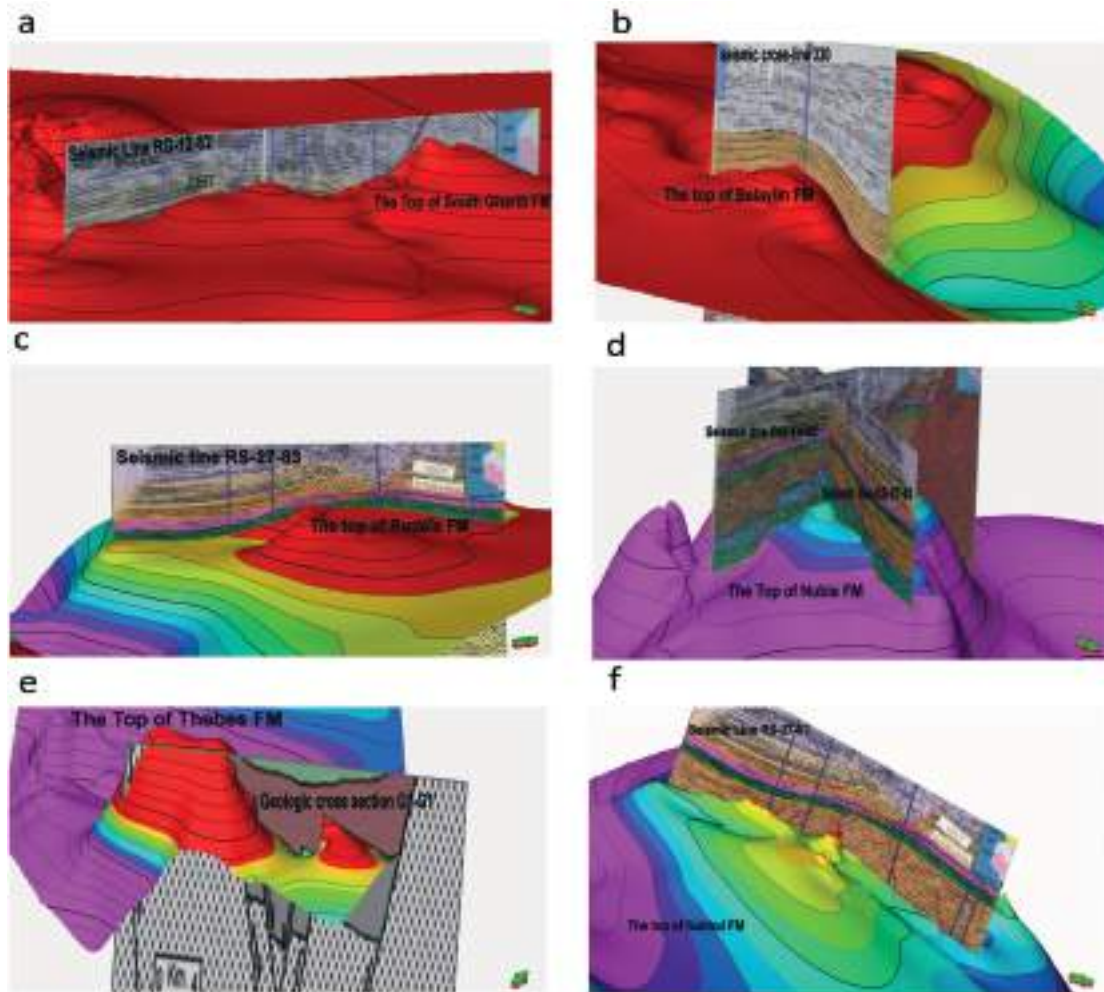


Figure 7. The tops. a – South Gharib Formation at seismic line RG-12-82; b – Belayim Formation at 3D seismic cross-line 330; c – Rudeis Formation at seismic line RS-27-83; d – Nubia Formation at crossing seismic lines RS27-83 and RG 14-82; e – Thebes Formation at geological cross section G1-G1'; f – Nukhul Formation at seismic line RS-27-83.

Рисунок 7. Вершины. а – Южно-Гарибская свита на сейсмической линии RG-12-82; б – Белайимская свита на 3D сейсмическом разрезе 330; с – Рудейская свита на сейсмической линии RS-27-83; д – Нубийская свита при пересечении сейсмических линий RS27-83 и RG 14-82; е – Фивская свита на геологическом разрезе G1-G1'; ф – Нухульская свита на сейсмической линии RS-27-83.

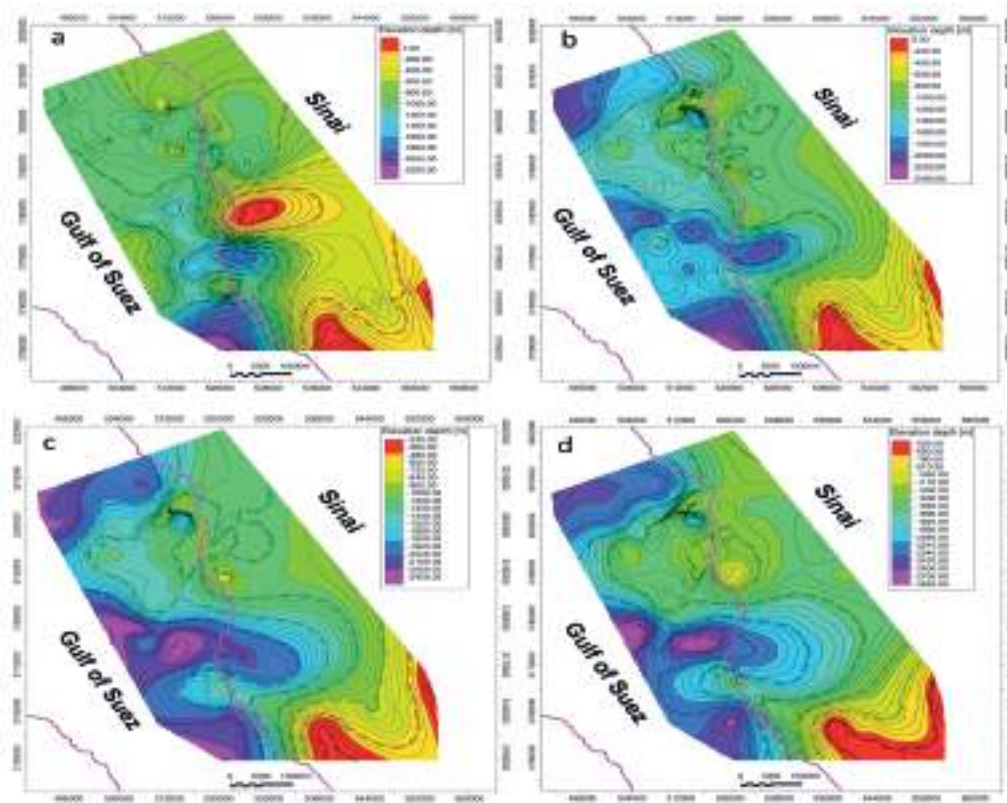


Figure 8. Structure contour maps: of a – the top Zeit Formation; b – the top South Gharib Formation; c – the top Belayim Formation; d – the top Kareem Formation of the study area.

Рисунок 8. Структурные контурные карты: а – вершина Зейт-формации; б – верхняя формация Южного Гариба; с – верхняя Белаймская свита; д – верхняя Каримская свита района исследования.

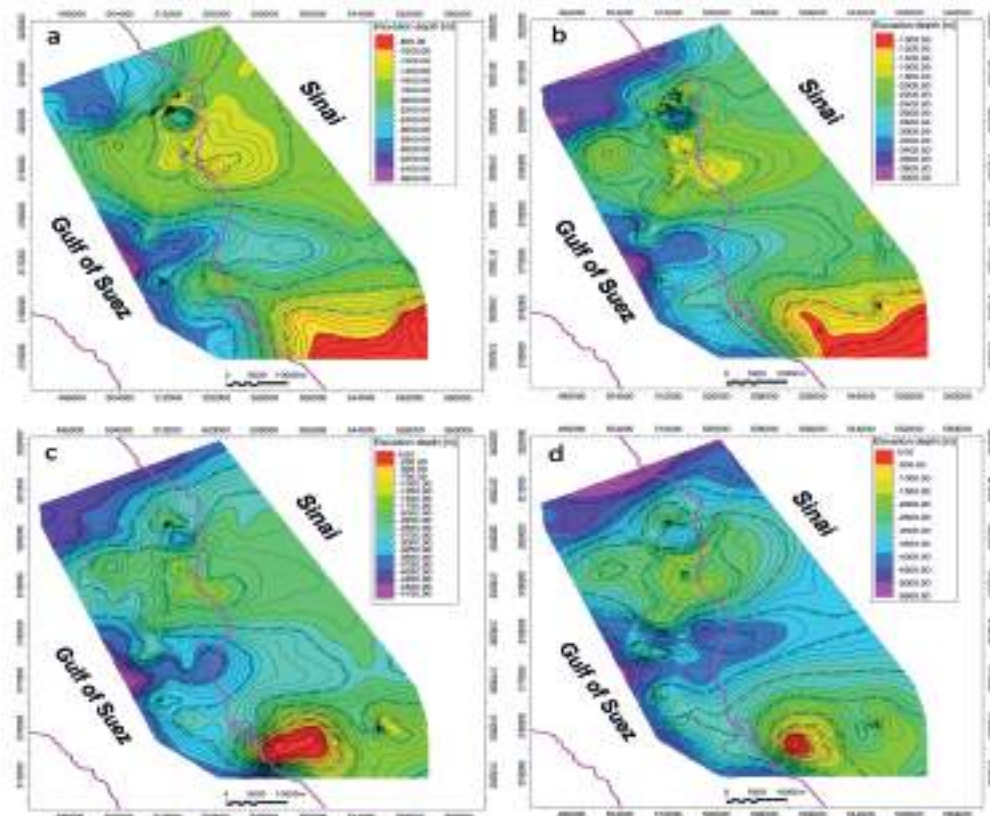


Figure 9. Structure contour map of: a – the top Rudeis Formation; b – the top Nukhul Formation; c – the top Thebes Formation; d – the top Matulla Formation of the study area.

Рисунок 9. Структура контурной карты: а – верхней Рудейской свиты; б – верхней Нухульской свиты; с – верхней Фивской свиты; д – кровля Матуллской свиты района исследования.

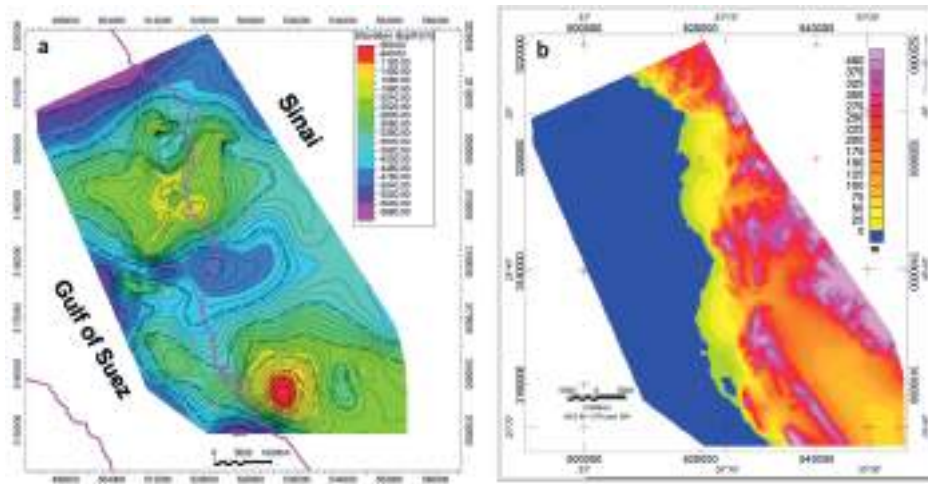


Figure 10. Structure and topographic maps. a – structure contour map of the top Nubia Formation; b – SRTM digital elevation model of the study area.

Рисунок 10. Структура и топографические карты. а – структура контурной карты верхней Нубийской свиты; б – SRTM цифровая модель рельефа района исследования.

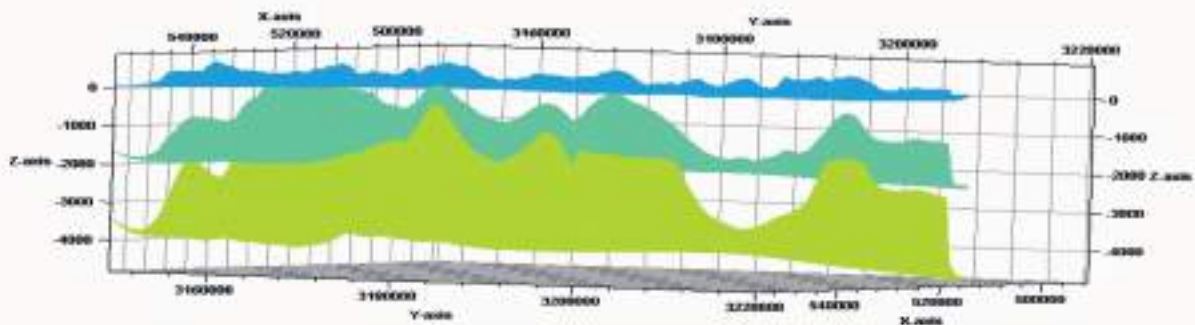


Figure 11. The skeletons of the eastern part of Gulf of Suez, Egypt.
Рисунок 11. Скелетные образования восточной части Суэцкого залива, Египет.

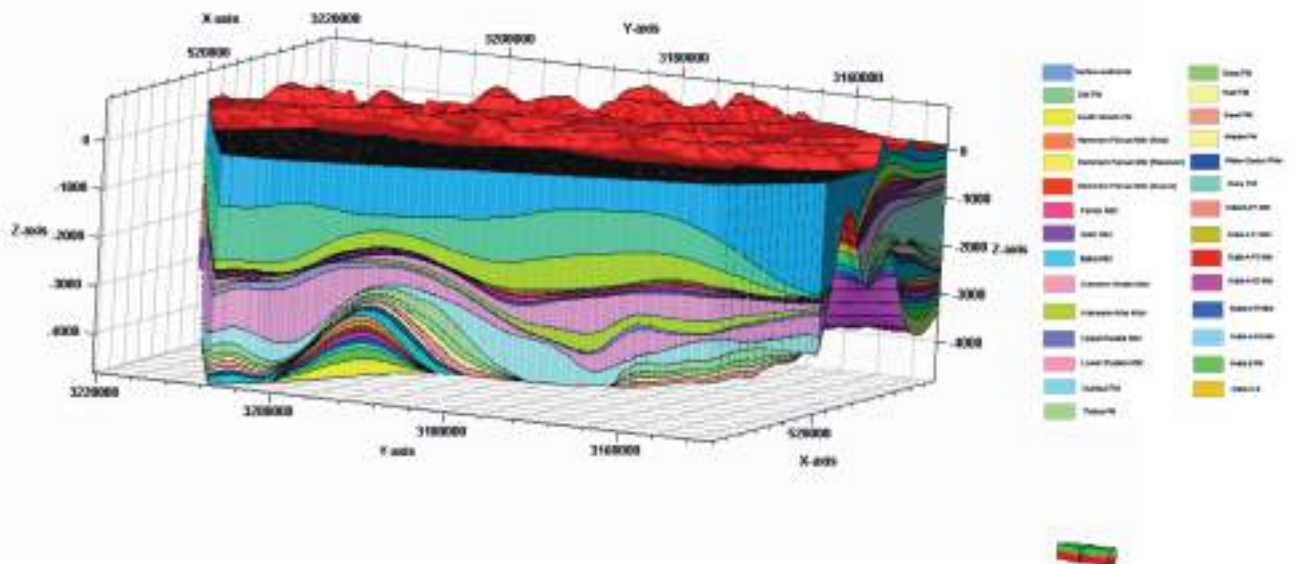


Figure 12. 3D based structure modelling using Petrel software of the study area.
Рисунок 12. Трёхмерное моделирование структуры с использованием программного обеспечения Petrel исследуемой территории.

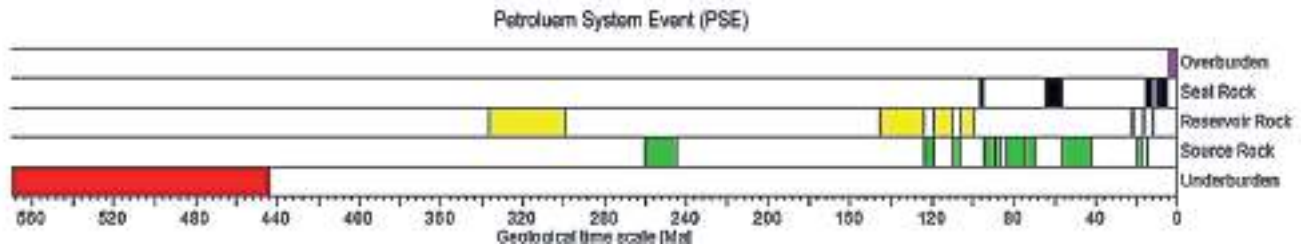


Figure 13. Petroleum system event chart, eastern part of Gulf of Suez, Egypt.
 Рисунок 13. Схема событий нефтяной системы, восточная часть Суэцкого залива, Египет.

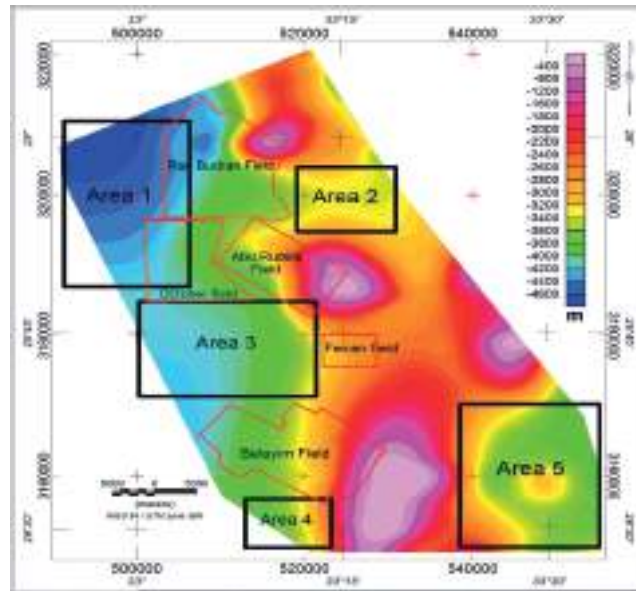


Figure 14. 3D magnetic depth map of the top basement rocks showing the promising zones for hydrocarbon of the study area.
 Рисунок 14. Трехмерная магнитная карта глубины верхних пород фундамента, показывающая перспективные зоны для углеводородов исследуемой территории.

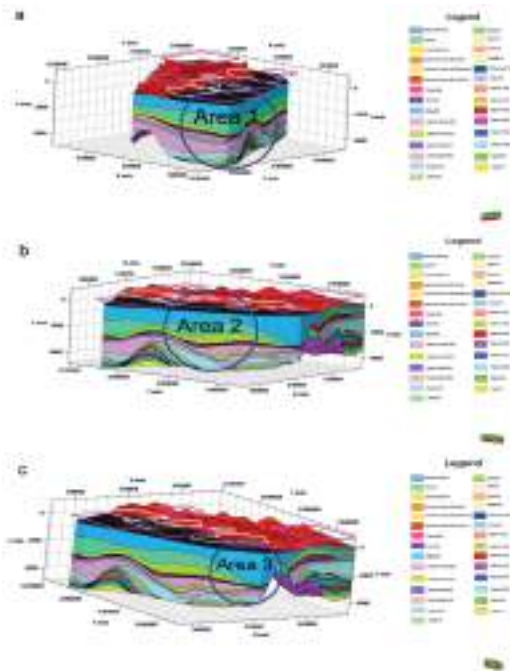


Figure 15. 3D modelling views of the promising zones 1, 2 and 3 using Petrel software, central eastern part of Gulf of Suez, Egypt.
 Рисунок 15. 3D-моделирование перспективных зон 1, 2 и 3 с использованием программного обеспечения Petrel, центральная восточная часть Суэцкого залива, Египет.

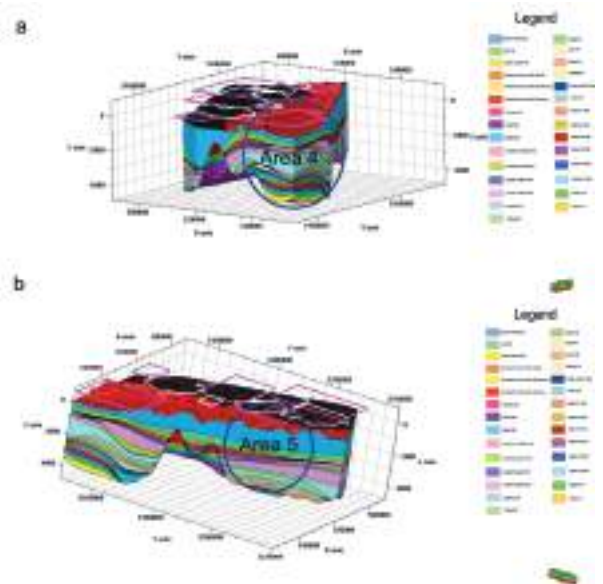


Figure 16. 3D modelling views of the promising zones 4 and 5 using Petrel software, central eastern part of Gulf of Suez, Egypt.
 Рисунок 16. 3D-моделирование перспективных зон 4 и 5 с использованием программного обеспечения Petrel, центральная восточная часть Суэцкого залива, Египет.

tentiality in other locations in the area is very high because of the existence of the sedimentary succession which allows trap forming characteristics (source, reservoir and sealing rocks). The boundaries of the currently known oil fields were plotted on top of the study area (Fig. 14) to predict new promising areas that may have potential for hydrocarbon and have not been fully explored.

The results of the 3D modelling (Fig. 15, 16) show that there are five locations within the study area that are considered to be basins, where the depth to the basement ranges from 3000 to 4500 m, in addition to the existence of a thick succession of sedimentary rocks overlaying the basement rocks. These areas need more attention through the use of 2D and 3D seismic surveys to explore new accumulations of hydrocarbons. The sedimentary succession for these areas includes seven reservoirs which are often overlain by seal rocks. These reservoirs can be divided into two types: pre-rift reservoirs and synrift reservoirs. Nubia A Sandstone-P1, Nubia A Sandstone-P2, Nubia A Sandstone-P3 are pre-rift reservoirs. The lithology of these reservoirs is mainly sandstone and each is overlain by a layer of shale which is considered a sealing rock. The Nukhul and upper Rudeis formations are synrift reservoirs. These reservoirs are sandstone and conglomerate that are overlain by a sealing rock.

Area (1) in the northwestern part of the study area (Fig. 15, a) is characterised by a great depth to the basement, which reaches 4500 m. The sedimentary succession in this area contains an adequate thickness of Belayim, Rudeis and Nubia A formations, which are considered good reservoirs. Oil and gas has been already discovered in these reservoirs in some other fields within the area, so we recommend undertaking 2D and 3D seismic surveys in this area to determine the probable presence of hydrocarbon. The depth to the basement in area (2), in the eastern part of the study area (Fig. 15, b), reaches 3000 m. Area (3) is in the central western part of the area to the south west of the Abu Rudeis field (Fig. 15, c). The depth to basement in this area is 4200 m, and the probability of the existence of hydrocarbon is increased in the Nukhul, Rudeis and Nubia A formations, as the lithology of these formations is good carrier rock, overlain by sealing rocks. In area (4) (Fig. 16, a), the depth to basement reaches 3600 m. This area is located in the southwestern part of the study area and it is located to the south of Belayim oil field which is one of the biggest oil fields in the GOS. The main reservoir in this field includes the Belayim and Nubia sandstones formations. One of the most important and promising areas in the study area is area (5) in the southeastern part (Fig. 16, b). No activity was undertaken in this area; however the probability of hydrocarbon accumulation may be very high. The depth to the basement in this area reaches 4100 m. 2D and 3D seismic surveys will be very useful so as to obtain detailed information about the subsurface geology, and a geochemical analysis to obtain information about the organic matter in the source rocks, where there is a thick sedimentary succession over the basement layer containing good multiple reservoirs, such as those in the Rudeis, Nukhul and Nubia formations. These reservoirs may be underlain by a good source rock. In a future study we will use this model and collect information about the heat flow, paleowater depth, organic matter, type of kerogen, and kinetics. Using this information we will be able to predict the locations and amounts of oil and gas that has accumulated in the reservoirs, by making a petroleum system model (PSM).

Conclusion

3D modelling of the airborne magnetic data was undertaken to delineate the depth to basement in the area under study. The results show that estimates of the depth to the basement varies reliably between 500 and 4700 m. 3D based structure model was created using Petrel software, depending on the available seismic sections and well data. The results of the 3D modelling show that there are five locations within the study area that are considered basins, where the depth to the basement varies between 3000 and 4500 m, and there is a good succession of sedimentary rocks overlaying the basement layer. These areas need more attention through 2D and 3D seismic survey to explore new accumulations of hydrocarbons. Making a petroleum system model (PSM) using the information about heat flow, paleowater depth, organic matter, type of kerogen, and kinetics will be very important for predicting the locations and amount of oil and gas accumulated in the reservoirs within the study area.

Acknowledgments

The authors would like to thank Nuclear Materials Authority for releasing the airborne magnetic data and for providing the necessary information and facilities to accomplish this work. Also, the authors would like to thank the Department of Geophysics at Saint Petersburg State University for allowing the use of the necessary software to accomplish this work.

REFERENCES

- McClay K. R., Nichols G. J., Khalil S. M., Darwish M., Bosworth W. 1998, Extensional tectonics and sedimentation, eastern Gulf of Suez, Egypt. In: B. H. Purser, D. W. J. Bosence (Eds.). Sedimentation and tectonics in Rift Basins Red Sea: Gulf of Aden. Dordrecht, Springer, pp. 223–238. https://doi.org/10.1007/978-94-011-4930-3_14
- Moustafa A. R. 2004, Explanatory Notes for the Geologic Maps of the Eastern Side of the Suez Rift (Western Sinai Peninsula). AAPG/Datapages, Incorporated GIS Series, Cairo.
- Abdeen M. M., Abdelmaksoud A. S. 2014, Aqaba-Levant transform-related faults in the Gulf of Suez rift: The Durba–Araba fault, Sinai Peninsula, Egypt. *Journal of African Earth Sciences*, vol. 97, pp. 342–356. <https://doi.org/10.1016/j.jafrearsci.2014.05.013>
- Moustafa A. R., Khalil S. M. 2017, Control of extensional transfer zones on syntectonic and post-tectonic sedimentation: implications for hydrocarbon exploration. *Journal of the Geological Society*, vol. 174, pp. 318–335. <https://doi.org/10.1144/jgs2015-138>
- Alsharhan A. S. 2003, Petroleum geology and potential hydrocarbon plays in the Gulf of Suez rift basin, Egypt. *AAPG Bulletin*, vol. 87, pp. 143–180.
- IHS E. 2006, Gulf of Suez Basin Monitor. Iris21 ID: 410900. IHS Energy.
- Caumon G., Carlier de Veslud C., Viseur S., Sausse J. 2009, Surface-based 3D modeling of geological structures. *International Association for Mathematical Geosciences, Math Geosci.*, vol. 41, pp. 927–945. <https://doi.org/10.1007/s11004-009-9244-2>
- Branets L. V., Ghai S. S., Lyons S. L., Xiao-Hui Wu. 2009, Challenges and technologies in reservoir modelling. *Communication in Computational Physics*, vol. 6, pp. 1–23. <https://doi.org/10.4208/cicp.2009.v6.p1> какая-то ошибка-не открывается
- Al-Baldawi B. A. 2015, Building a 3D geological model using Petrel Software for Asmari Reservoir, South Eastern Iraq. *Iraqi Journal of Science*, vol. 56, pp. 1750–1762.
- Shimanskiy S. V., Tarshan A. 2019, Basement configuration depth methods of airborne magnetic data in the eastern Gulf of Suez, Egypt. *News of the Ural State Mining University Journal*, vol. 53, issue 1, pp. 7–17. <https://doi.org/10.21440/2307-2091-2019-1-7-17>
- Mokhles A., Mostafa M., Desouky I., Pepe F. 2003, Impact of 3D seismic technique on production optimization in Belayim Land Field, Central Gulf of Suez, Egypt. The Offshore Mediterranean Conference: An Exhibition in Ravenna, Italy, March 26–28.
- Zahra H. S., Nakhla A. M. 2015, Deducing the subsurface geological conditions and structural framework of the NE Gulf of Suez area, using 2-D and 3-D seismic data. *NRIAG Journal of Astronomy and Geophysics*, vol. 4, pp. 64–85. <https://doi.org/10.1016/j.nrjag.2015.04.003>
- Zahra H. S., Nakhla A. M. 2016, Structural interpretation of seismic data of Abu Rudeis-Sidri area, Northern Central Gulf of Suez, Egypt. *NRIAG Journal of Astronomy and Geophysics*, vol. 5, pp. 435–450. <https://doi.org/10.1016/j.nrjag.2016.09.002>
- Rabeh T., Miranda J. M., Carvalho J., Bocin A. 2009, Interpretation case study of the Sahl El Qaa area, southern Sinai Peninsula, Egypt. *Ge-*

ophysical Prospecting, vol. 57, issue 3, pp. 447–459. <https://doi.org/10.1111/j.1365-2478.2008.00747.x>

15. Tarshan A., Shimanskiy S. 2019, Petroleum system modelling and identification of promising oil and gas bearing objects in the eastern part of the Gulf of Suez, Egypt. *Russian Journal of Earth Sciences* [In press].
16. Abou Shagar S. 2006, Source rock evaluation of some intervals in the Gulf of Suez area, Egypt. *Egyptian Journal of Aquatic Research*, vol. 32, pp. 70–87.
17. Lashin A., Al-Arifi N., Abu Ashour N. 2011, Evaluation of the ASL and Hawara formations using seismic- and log-derived properties, October Oil Field, Gulf of Suez, Egypt. *Arabian Journal of Geosciences*, vol. 4, issue 3-4, pp. 365–383. <https://doi.org/10.1007/s12517-009-0065-x>
18. Naglaa M. S., Nabil S. A., Ahmed E. K. M. 2013, Hydrocarbon generating basins and migration pathways in the Gulf of Suez, Egypt. *Life Science Journal*, vol. 10, pp. 229–235.
19. Atia H. M. 2014, An integrative modeling of Ras Budran Field, Gulf of Suez, Egypt. Unpublished MSc. Thesis. Mansoura: Mansoura University, Egypt.
20. Mohamed H. B. 2014, Radiogenic heat production and reservoir properties of Rudeis Formation in Belayim Marine oil field, Gulf of Suez, Egypt. Unpublished MSc. Thesis. Cairo: Ain Shams University. Egypt.
21. Al-Atta M. A., Issa G. I., Ahmed M. A., Afife M. M. 2014, Source rock evaluation and organic geochemistry of Belayim Marine Oil Field, Gulf of Suez, Egypt. *Egyptian Journal of Petroleum*, vol. 23, issue 3, pp. 285–302. <https://doi.org/10.1016/j.ejpe.2014.08.005>
22. Abu Al-Atta M.A. 2015, Hydrocarbon exploration and tectonic evolution of Belayim Marine Oil Field, Gulf of Suez, Egypt. Unpublished M.Sc. Thesis, Mansoura: Mansoura University, Egypt.
23. Afife M. M., Al-Atta M. A., Ahmed M. A., Issa G. I. 2016, Thermal maturity and hydrocarbon generation of the Dawi Formation, Belayim Marine Oil Field, Gulf of Suez, Egypt: a 1D basin modelling case study. *Arabian Journal of Geosciences*, vol. 9, pp. 1–31. <https://doi.org/10.1007/s12517-016-2320-2>
24. El Diasty W. Sh., Abo Ghonaim A. A., Mostafa A. R., El Beialy S. Y., Edwards K. J. 2016, Biomarker characteristics of the Turonian–Eocene succession, Belayim oil fields, central Gulf of Suez, Egypt. *Journal of the Association of Arab Universities for Basic and Applied Sciences*, vol. 19, issue 1, pp. 91–100. <https://doi.org/10.1016/j.jaubas.2014.06.001>

The article was received on February 20, 2019

Трехмерное глубинное структурное моделирование центральной восточной части Суэцкого залива, Египет

Ахмед ТАРШАН^{1, 2*},
Сергей Владимирович ШИМАНСКИЙ^{1**},
Мамдух М. АБДИН^{3***}

¹Санкт-Петербургский государственный университет, Санкт-Петербург, Россия

²Управление по ядерным материалам, Каир, Египет

³Национальное управление по дистанционному зондированию и космической науке, Каир, Египет

Актуальность. Построение трехмерной (3D) геологической модели на основе полевых материалов и данных о строении земли является важной задачей в геологических и геофизических исследованиях.


Целью данного исследования является построение трехмерной структурной модели центральной восточной части Суэцкого залива, Египет. При построении модели использовались данные о сейсмических разрезах и скважинах. Каждый горизонт (на каждом сейсмическом разрезе) был точно оцифрован с использованием программного обеспечения Petrel для создания карты структуры глубины для каждого горизонта. Слой фундамента был сформирован с использованием данных аэромагниторазведки исследуемой области. Использовался инверсионный код GM-SYS-3D для предположения о магнитной восприимчивости комплекса пород фундамента. Оценки глубины до основания достоверно варьировались от 500 до 4700 м. Данные по 24 пробуренным скважинам в пределах области были использованы для определения толщины и ориентации слоев между горизонтами трехмерной модели сетки. Модель, состоящая из 29 слоев, включая топографию и слои фундамента, была создана с использованием программного обеспечения Petrel.

Результаты 3D-модели показывают, что область исследования имеет многоколлекторный характер с несколькими продуктивными предрифтовыми и синрифтовыми коллекторами. В ней содержатся семь резервуаров, перекрытых флюидоупорными породами и подстилаемых материнскими породами. Наличие углеводородов в этих резервуарах было продемонстрировано на некоторых месторождениях в этом районе. Кроме того, для детальной 2D и 3D сейсморазведки рекомендованы пять новых мест, так как в них может присутствовать углеводород.

Ключевые слова: 3D моделирование, карты глубинной структуры, горизонты и слои, Суэцкий залив, Египет.

Статья поступила в редакцию 20 февраля 2019 г.

* ahmed_ramadan_geo@hotmail.com

 <https://orcid.org/0000-0001-9710-9392>

** s.shimanskii@spbu.ru

 <https://orcid.org/0000-0002-5403-5220>

*** mamdouh.abdeen@narss.sci.eg

 <https://orcid.org/0000-0001-8863-1322>